Angular velocity variations and stability of spatially explicit prey-predator systems

Refael Abta and Nadav M. Shnerb
Department of Physics, Bar-Ilan University, Ramat-Gan 52900 Israel
(Received 14 December 2006; published 23 May 2007)

The linear instability of Lotka-Volterra orbits in the homogenous manifold of a two-patch system is analyzed. The origin of these orbits instability in the absence of prey migration is revealed to be the dependence of the angular velocity on the azimuthal angle; in particular, the system desynchronizes at the exit from the slow part of the trajectory. Using this insight, an analogous model of a two coupled oscillator is presented and shown to yield the same type of linear instability. This enables one to incorporate the linear instability within a recently presented general framework that allows for comparison of all known stabilization mechanisms and for simple classification of observed oscillations.

DOI: 10.1103/PhysRevE.75.051914 PACS number(s): 87.23.Cc, 05.45.Xt, 02.50.Ey

Population oscillations in prey predator systems, as predicted by the Lotka-Volterra equations [1], are known to be unstable with respect to additive and multiplicative noise. This instability must lead to the extinction of one of the interacting species, a fact that has been confirmed in various experiments for well-mixed populations [2]. The persistence of natural prey-predator and host-parasitoid systems is thus commonly attributed to their spatial structure, such that migration between desynchronized patches yields an inward flow toward the coexistence fixed point and is responsible for the sustainability of the oscillations [3]. In fact, spatially extended systems tend to support finite amplitude oscillation [4]. The stabilization of such oscillations is considered to be a major factor affecting species conservation and ecological balance [5]. Thus, a major challenge is to understand the conditions for the appearance of desynchronization in diffusively coupled patches, since diffusion tends to synchronize these patches so that after a while the whole system flows to the well-mixed, unstable limit [6]. One of the solutions to that problem was presented by Jansen [7–9]. It turns out that the trajectories far from the fixed point become unstable if the inter-patch migration rate of the predator is much larger than that of the prey. Jansen used Floquet analysis to show that instability. In this paper, we try to elucidate the underlying mechanism that yields Jansen's instability, to generalize it in the framework of the recently presented coupled oscillator model, and to discuss the conditions under which one may observe the stabilizing effect of Jansen's mechanism, like oscillation amplitude that grows under noise until it reaches the first unstable orbit.

The Lotka-Volterra predator-prey system is a paradigmatic model for oscillations in population dynamics [1]. It describes the time evolution of two interacting populations: a prey (b) population that grows with a constant birth rate σ in the absence of a predator (the energy resources consumed by the prey are assumed to be inexhaustible), while the predator population (a) decays (with death rate μ) in the absence of a prey. Upon encounter, the predator may consume the prey with a certain probability. Following a consumption event, the predator population grows and the prey population decreases. For a well-mixed population, the corresponding partial differential equations are

$$\frac{\partial a}{\partial t} = -\mu a + \lambda_1 ab,$$

$$\frac{\partial b}{\partial t} = \sigma b - \lambda_2 ab, \tag{1}$$

where λ_1 and λ_2 are, correspondingly, the relative increase (decrease) of the predator (prey) populations due to the interaction between species.

The system admits two unstable fixed points: the absorbing state $a=b=0$ and the state $a=0$, $b=\infty$. There is one marginally stable fixed point at $\bar{a}=\sigma/\lambda_2$, $\bar{b}=\mu/\lambda_1$. Local stability analysis yields the eigenvalues $\pm i\sqrt{\mu\sigma}$ for the stability matrix. Moreover, even beyond the linear regime, there is neither convergence nor repulsion. Using logarithmic variables $z=\ln(a), q=\ln(b)$, Eqs. (1) take the canonical form $\dot{z}=\partial H/\partial q$, $\dot{q}=-\partial H/\partial z$, where the conserved quantity H (in the ab representation) is

$$H = \lambda_1 b + \lambda_2 a - \mu \ln(a) - \sigma \ln(b). \tag{2}$$

The phase space is, thus, segregated into a collection of nested one-dimensional trajectories, where each one is characterized by a different value of H, as illustrated in Fig. 1. Given a line connecting the fixed point to one of the "walls"

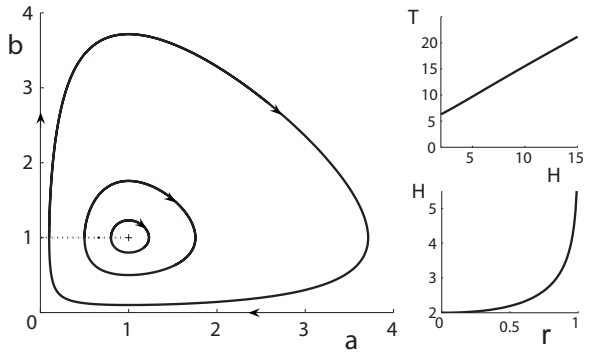

FIG. 1. The Lotka-Volterra phase space (left panel) admits a marginally stable fixed point surrounded by close trajectories (three of these are plotted). Each trajectory corresponds to single H defined in Eq. (2), where H increases monotonically along the (dashed) line connecting the center with the $a=0$ wall, as shown in the lower-right panel. In the upper-right panel, the period of a cycle T is plotted against H, and is shown to increase almost linearly from its initial value $T=2\pi/\sqrt{\mu\sigma}$ close to the center.

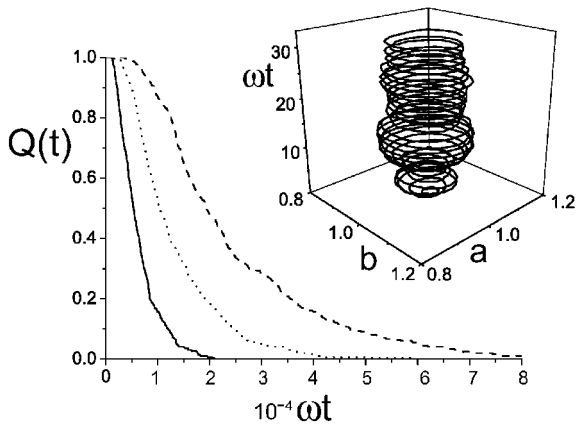

FIG. 2. The survival probability $Q(t)$ is plotted versus time for a single-patch, noisy LV system. Equations (1) (with the symmetric parameters) were integrated numerically (Euler integration with time step 0.001), where the initial conditions are at the fixed point $a=b=1$. At each time step, a small random number, $\eta(t)\Delta t$, was added to each population density, where $\eta(t) \in [-\Delta, \Delta]$. A typical phase space trajectory, for $\Delta=0.5$, is shown in the inset. The system "dies" when the trajectory hits the walls $a=0$ or $b=0$. Using 300 different noise histories, the survival probability is shown here for $\Delta=0.5$ (full line), $\Delta=0.3$ (dotted line), and $\Delta=0.25$ (dashed line). Clearly, the survival probability decays exponentially at long times, $Q(t) \sim \exp(-t/\tau)$. As expected for a random walk with absorbing boundary conditions, $1/\tau$ scales with Δ^2.

(e.g., the dashed line in the phase space portrait, Fig. 1), H is a monotonic function on that line, taking its minimum, $H_{\min}$, at the marginally stable fixed point (center) and diverging on the wall. Note that, without loss of generality, we employ the symmetric parameters $\mu=\sigma=\lambda_1=\lambda_2=1$ or, if needed, assume $\lambda_1=\lambda_2=\lambda$; the results presented hereon are generic and independent of the parameters involved. The corresponding phase space, along with the dependence of H on the distance from the center and a plot of the oscillation period vs H, are represented in Fig. 1).

Given the integrability of that system, the effect of noise is quite trivial: if a and b randomly fluctuate in time (e.g., by adding or subtracting small amounts of population during each time step), the system wanders between trajectories, thus performing some sort of random walk in H with "repelling boundary conditions" at $H_{\min}$ and "absorbing boundary conditions" on the walls (as negative densities are meaningless, the "death" of the system is declared when the trajectory hits the zero population state for one of the species). This result was emphasized by Gillespie [10] for the important case where intrinsic stochastic fluctuations are induced by the discrete character of the reactants. In that case, the noise is multiplicative (proportional to the number of particles), and the system flows away from the center and eventually hits one of the absorbing states at (0,0) or $(0,\infty)$. The corresponding situation for a single patch Lotka-Volterra system with additive noise is demonstrated in Fig. 2, where the survival probability $Q(t)$ (the probability that a trajectory does not hit the absorbing walls within time t) is shown for different noise amplitudes.

The Lotka-Volterra system on spatial domains has been investigated, usually in a form of diffusively coupled patches, during the last decades. Any patch is assumed to be well mixed, and the flow of the reactants from one patch to its neighbors is governed by the density gradient. Clearly, any system of that type, independent of its spatial topology (either regular lattice of some dimensionality or some sort of network without isolated nodes) admits an infinite number of solutions that correspond to *synchronous* oscillations of the whole system along one of the H trajectories, where the diffusion has no role as there are no population gradients. The simplest example is the two-patch system [11], described by

$$\frac{\partial a_1}{\partial t} = -\mu a_1 + \lambda a_1 b_1 + D_a(a_2 - a_1),$$

$$\frac{\partial a_2}{\partial t} = -\mu a_2 + \lambda a_2 b_2 + D_a(a_1 - a_2),$$

$$\frac{\partial b_1}{\partial t} = \sigma b_1 - \lambda a_1 b_1 + D_b(b_2 - b_1),$$

$$\frac{\partial b_2}{\partial t} = \sigma b_2 - \lambda a_2 b_2 + D_b(b_1 - b_2). \tag{3}$$

Here the invariant manifold is the two-dimensional subspace $a_1=a_2, b_1=b_2$. The diffusion, of course, suppresses fluctuations and stabilizes the invariant manifold; one may thus expect that the single-patch dynamics also capture the main features of the extended system, and that the system behaves like a random walker in the invariant manifold (with a rescaled noise) and hits the absorbing walls after some characteristic time, τ, where τ scales linearly with the noise strength Δ^2.

As a first hint for a stabilizing mechanism, let us consider the total H (in symmetric parameters),

$$H_T \equiv H_1 + H_2 = a_1 + a_2 + b_1 + b_2 - \ln(a_1 a_2 b_1 b_2). \tag{4}$$

With the deterministic dynamics (3), H_T is a *monotonously decreasing* quantity in the non-negative population regime,

$$\frac{dH_T}{dt} = -D_a\left[\frac{(a_1 - a_2)^2}{a_1 a_2}\right] - D_b\left[\frac{(b_1 - b_2)^2}{b_1 b_2}\right] < 0. \tag{5}$$

Accordingly, if an orbit on the invariant manifold becomes unstable, the flow will be inward and the population oscillations stabilizes. While if $D_a=D_b$, the stability properties of an orbit on the invariant manifold are identical to the stability properties of the corresponding single-patch orbit [12]; if the diffusion of both species is different, there is a possibility for unstable orbits on the homogenous plane. This option was materialized by Jansen [7], who considered the set of Eqs. (3) in the limit $D_b=0$, so that only the predator undergoes diffusion. With the transformation

$$A = \frac{a_1 + a_2}{2}, \quad B = \frac{b_1 + b_2}{2},$$

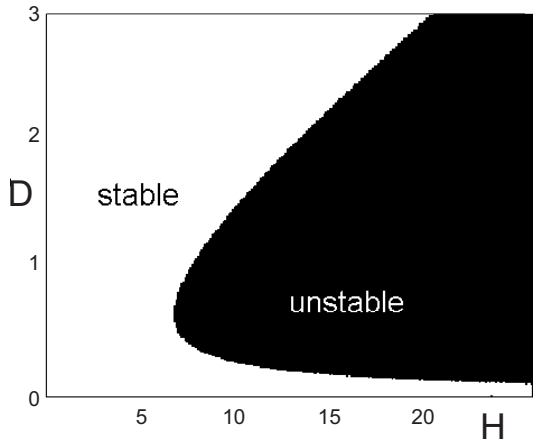

FIG. 3. Stability diagram for phase space orbits (ordered by their conserved quantity H) for different values of predator diffusion D_a, where $D_b=0$.

$$\delta = \frac{a_1 - a_2}{2}, \quad \theta = \frac{b_1 - b_2}{2}, \tag{6}$$

one recognizes the homogenous AB manifold and that the δ θ coordinates measure the deviation from that manifold (the heterogeneity of the population). In these coordinates the system satisfies

$$\frac{\partial A}{\partial t} = -\mu A + \lambda AB + \lambda \delta\theta,$$

$$\frac{\partial B}{\partial t} = \sigma B - \lambda AB + \lambda \delta\theta,$$

$$\frac{\partial \delta}{\partial t} = -\mu\delta + \lambda A\theta + \lambda B\delta - 2D_a\delta,$$

$$\frac{\partial \theta}{\partial t} = \sigma\theta - \lambda A\theta - \lambda B\delta - 2D_b\theta. \tag{7}$$

Linearizing around the homogenous manifold, the AB dynamic is equivalent to that of a single patch:

$$\dot{A} = -\mu A + \lambda AB,$$

$$\dot{B} = \sigma B - \lambda AB, \tag{8}$$

and the $\delta-\theta$ linearized dynamic is

$$\frac{\partial}{\partial t}\begin{pmatrix}\delta\\ \theta\end{pmatrix} = \begin{pmatrix}-\mu + \lambda B - 2D_a & \lambda A\\ -\lambda B & \sigma - \lambda A - 2D_b\end{pmatrix}\begin{pmatrix}\delta\\ \theta\end{pmatrix}. \tag{9}$$

One may thus calculate the eigenvalues of the Floquet operator for one period along an orbit of the homogenous manifold (8). The resulting stability diagram, first obtained by Ref. [7], is shown in Fig. 3.

Our first mission is to intuitively explain Jansen's results. First, we notice that the angular velocity along a single Lotka-Volterra orbit is not fixed. Figure 4 emphasizes the angular velocity gradient along an orbit. While the inner trajectories (close to the fixed point) are almost harmonic with constant angular velocity, the eccentric large H orbits admit large variations. In particular, the motion in the dilute population region [close to the unstable empty fixed point (0,0)] is very slow, while in the dense population region the angular velocity is large.

Following the caricature of an orbit in Fig. 5, we can explain the source of the instability. For a two-patch system, if one patch is at point A along the orbit and the other patch at B, since the A patch is moving faster along the line it will get closer and closer to B during their flow toward the slow region. The diffusion of the prey plays no role along this branch, since the prey density is almost equal, while the predator diffusion may only strengthen that effect. Thus, the two patches must (almost) synchronize along this branch.

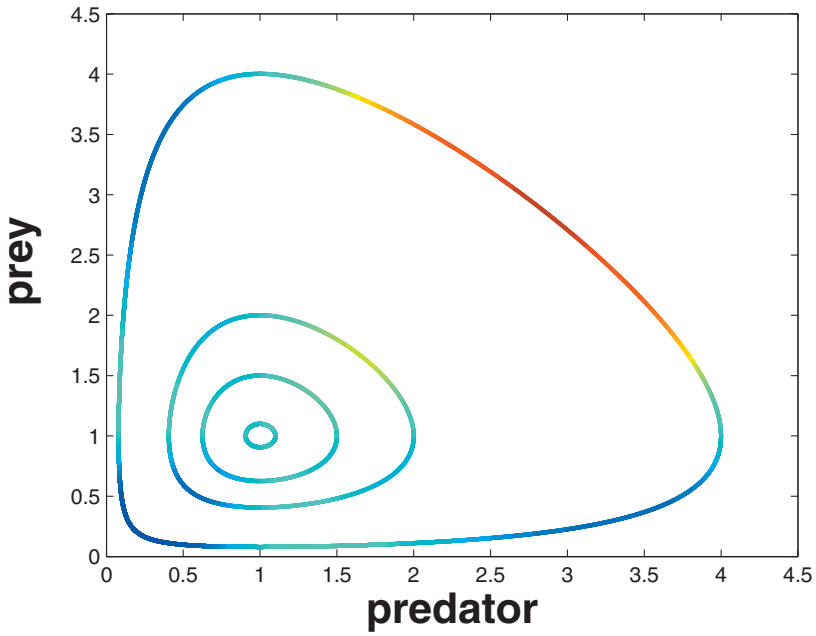

FIG. 4. (Color) The angular velocity along some orbits of the Lotka-Volterra dynamic. Fast regions marked in red, slow regions are blue. Clearly, the dynamics is slowest when the populations of both species are diluted, and fastest along the dense region in the upper-right "shoulder." Note that the velocity gradient along an orbit increases with H.

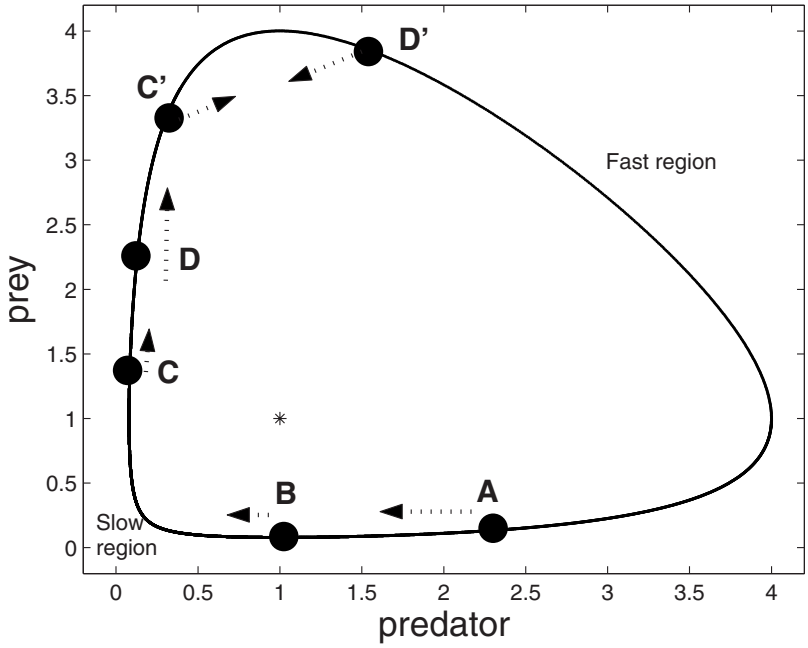

FIG. 5. An orbit of the LV dynamics and its fast and slow regions. As explained in the text, with no prey migration the two patches desynchronize in the *CD* region, thus predator diffusion causes a flow toward the fixed point and stabilizes the oscillations.

The situation is completely different in the exit from the slow region. The patch at D moves much faster than that at C, so they will *desynchronize*. As the predator density along this branch is almost constant, the only factor that may avoid desynchronization is the prey migration. In the absence of prey migration, the two patches reach the points C′ and D′, where the predator migration produces an inward flow. Figure 6 is now well understood: the inward flow happens when the desynchronization interferes with the predator diffusion, as explained.

Let us consider now Jansen's instability in the framework of the coupled nonlinear oscillator toy model, recently presented in Refs. [13,15] as a generic tool for the investigation of oscillation stability in diffusively coupled metapopulations. With the intuition gathered from the above example, we want to consider diffusively coupled orbits where the angular velocity depends on the radial angle and the diffusing species density is changing along the slowing branch. The following equations,

$$\frac{\partial x_1}{\partial t} = \omega(\theta_1) y_1 + D_x(x_2 - x_1),$$

$$\frac{\partial x_2}{\partial t} = \omega(\theta_2) y_2 + D_x(x_1 - x_2),$$

$$\frac{\partial y_1}{\partial t} = -\omega(\theta_1) x_1 + D_y(y_2 - y_1),$$

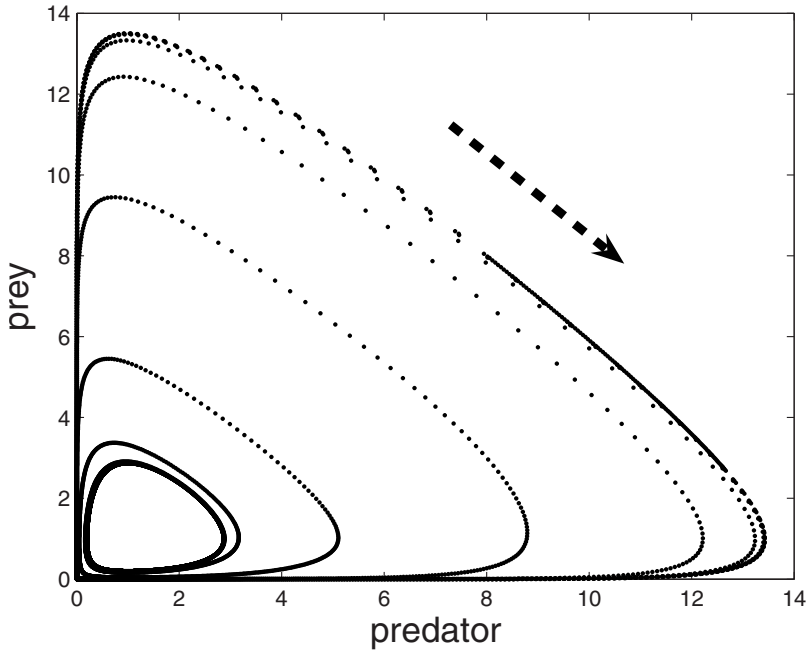

FIG. 6. Phase portrait of the inward flow in the homogenous manifold (average prey density vs average predator density) for two-patch LV system with no prey diffusion and $D_{\text{predators}}=1$. Clearly, the inward flow happens in the $C'-D'$ region of Fig. 5, where the desynchronization along the *CD* branch interferes with the predator diffusion. There is almost no inward motion along the rest of the orbit.

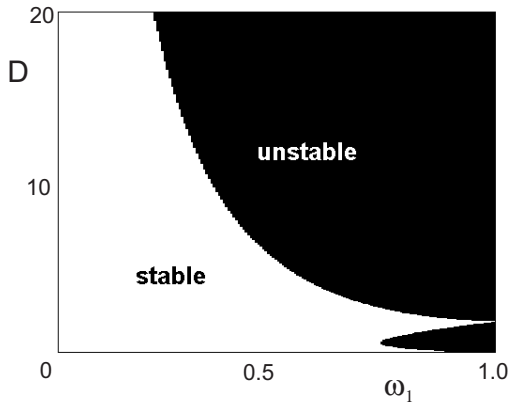

FIG. 7. Stability diagram in the $\omega_1 - D_x$ plane for the Floquet operator (same as Fig. 3) for the coupled oscillator system described by Eqs. (10) with $D_y=0$. The two unstable regions correspond to different signs of the Floquet unstable eigenvalue, as explained in the text.

$$\frac{\partial y_2}{\partial t} = -\omega(\theta_2)x_2 + D_y(y_1 - y_2), \tag{10}$$

will satisfy these conditions for $D_x=D$, $D_y=0$ and

$$\omega = \omega_0 + \omega_1 \cos\left(\theta - \frac{\pi}{4}\right). \tag{11}$$

Using $(i \in 1,2)$

$$r_i^2 = x_i^2 + y_i^2, \quad \theta_i = \arctan\left(\frac{y_i}{x_i}\right),$$

$$\dot{r} = \frac{(x\dot{x} + y\dot{y})}{r}, \quad \dot{\theta} = \frac{(x\dot{y} - y\dot{x})}{r^2}, \tag{12}$$

and

$$r = r_2 - r_1, \quad R = r_2 + r_1,$$

$$\phi = \theta_2 - \theta_1, \quad \Phi = \theta_2 + \theta_1, \tag{13}$$

one finds that the flow in the invariant manifold satisfies

$$\dot{R} = 0,$$

$$\dot{\Phi} = \omega(\theta_1) + \omega(\theta_2), \tag{14}$$

while the linearized equations for the desynchronization amplitude, r and the desynchronization angle, ϕ, satisfy

$$\frac{\partial}{\partial t}\begin{pmatrix}\phi\\ r\end{pmatrix} = \begin{pmatrix} 2\omega'(\Phi/2) - 2D_x\cos^2(\Phi/2) & \dfrac{D_x \sin\Phi}{R} \\ \dfrac{-D_x R \sin\Phi}{2} & -2D_x \sin^2(\Phi/2)\end{pmatrix} \times \begin{pmatrix}\phi\\ r\end{pmatrix}. \tag{15}$$

Using the Floquet operator technique to analyze the stability of an orbit by integrating (15) along a close trajectory of (14), one finds the stability map presented in Fig. 7, where

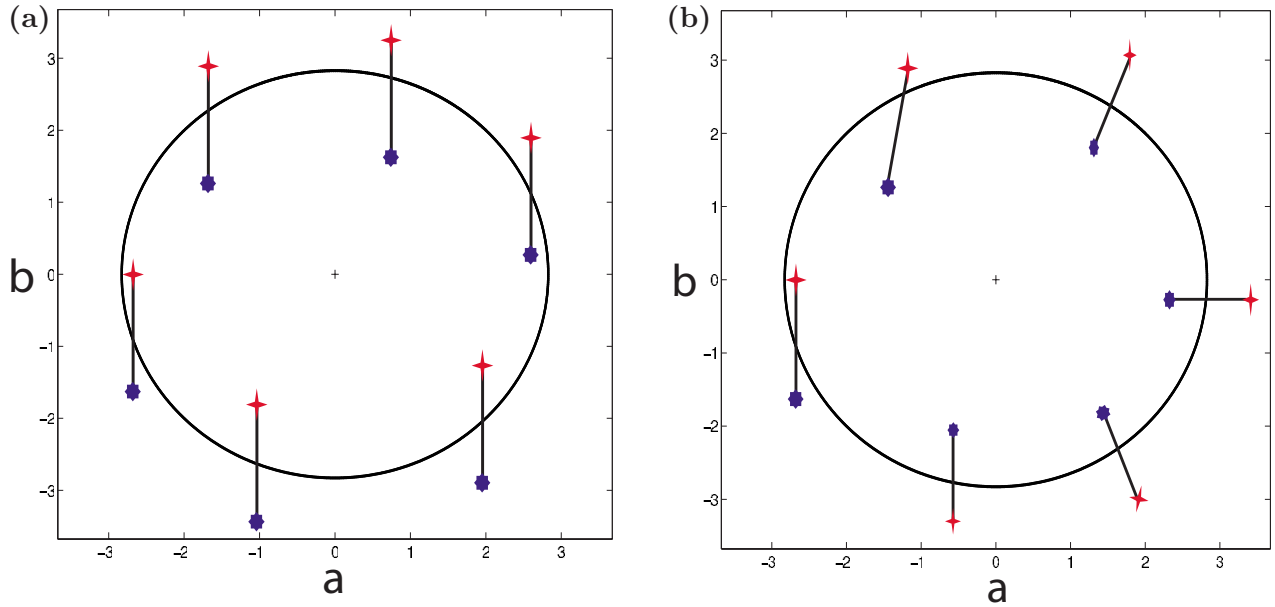

FIG. 8. (Color online) An illustration of the trajectories of two diffusively-coupled patches, with slightly different initial conditions, projected on the invariant manifold. In the strong coupling case (left panel), the strong predator diffusion forces the two points to be on the same vertical line (same predator concentration) along the orbit, hence the phase of the Floquet eigenvalue inverted twice along the trajectory, yielding a positive eigenvalue. In the small diffusion limit, the patches possess equal predator density only in the slow portion of the orbit, when the intra-patch dynamic is slow with regard to the migration. This leads to trajectories like those illustrated in the right panel (points connected by "rod" stand for the population density in equal times), where only one sign change happens and the Floquet eigenvalue is positive.

the parameter H of Fig. 3 is now replaced by ω_1, which measures the "eccentricity" of the angular velocity along a circular path. Here, two unstable regions appear, for large and small D_x.

It is interesting to point out that, in the high D_x region, the unstable eigenvalue is positive, while in the small D_x unstable region, it takes negative values. The reason for that is the effect of predator migration. If the effect of migration is large, in comparison with the intra-patch dynamics, the two patches should admit (almost) the same predator density, and the corresponding points in the $2d$ phase portrait should stay on the same vertical line (same "x" coordinate). The trajectories of the two points representing the patches along an orbit are thus similar to the transport of a vertical rod along a circle, keeping the center of the rod on the circular trajectory: the two ends switch their role *twice* (the inner becomes the outer and vice versa) so the rod returns to its original state after a full cycle (see Fig. 8, left panel). In the low diffusion range, on the other hand, the points remain on a vertical line only close to the slow portion of the orbit, where they switch once, but in the fast region they support different predator populations, so the "rod" completes its cycle in opposite "phase" (see Fig. 8, right panel).

We now turn to our last point, a comparison of this stabilizing mechanism with the nonlinear, noise induced mechanism recently presented by us [13]. The stability mechanism of Ref. [13] involved with the *amplitude dependence* of the angular velocity (see the upper right panel of Fig. 1), works as well for a system of equal prey and predator migration rates and is not based on a linear instability of an orbit. One may then ask how to make a distinction between these two mechanisms in real systems.

In order to make a distinction between amplitude-induced stability [13] and angular-induced stability [7], one should compare the corresponding radius of oscillations, where the dominant mechanism corresponds to the smaller radius. The

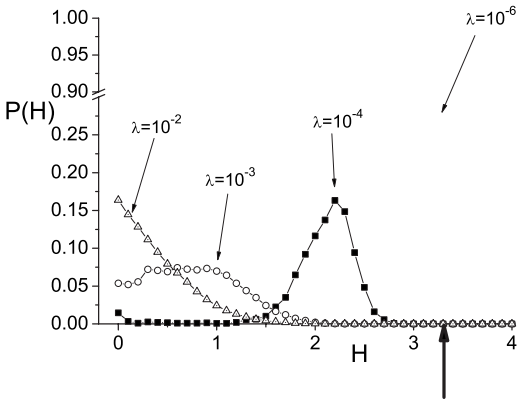

FIG. 9. The probability density to be at certain trajectory $P(H)$ vs H for coupled two-patch LV system with demographic stochasticity for different population sizes. The conserve quantity, H [Eq. (2)], was rescaled such that, at the coexistence point, its value is zero. All cases were simulated for $\mu=\sigma=1$, so the population (number of individuals in each of the species) at the coexistence fixed point is $1/\lambda$. Noise is proportional to the square root of the population, to mimic the effect of demographic stochasticity. The diffusion value $D=1$ was chosen as it corresponds to the smallest amplitude of the last stable orbit and is way too large to allow amplitude desynchronization (see Ref. [13]). For small populations the effect of noise is relatively large and the amplitude dependence of the frequency is the dominant stabilizing mechanism, while for large populations $P(H)$ concentrates around the first unstable trajectory (its location is marked by an arrow).

amplitude synchronization prediction is that the oscillation radius scales like $D/(\omega')^2$, where $\omega' \equiv \partial\omega/\partial r$ is the frequency gradient along the oscillations amplitude (see Fig. 1, upper-right panel). This result should be compared with the instability radius of [7], and for small migration rates ($D \sim 0.01$) it is smaller in few orders of magnitude. It thus seems that the angular induced instability will be relevant

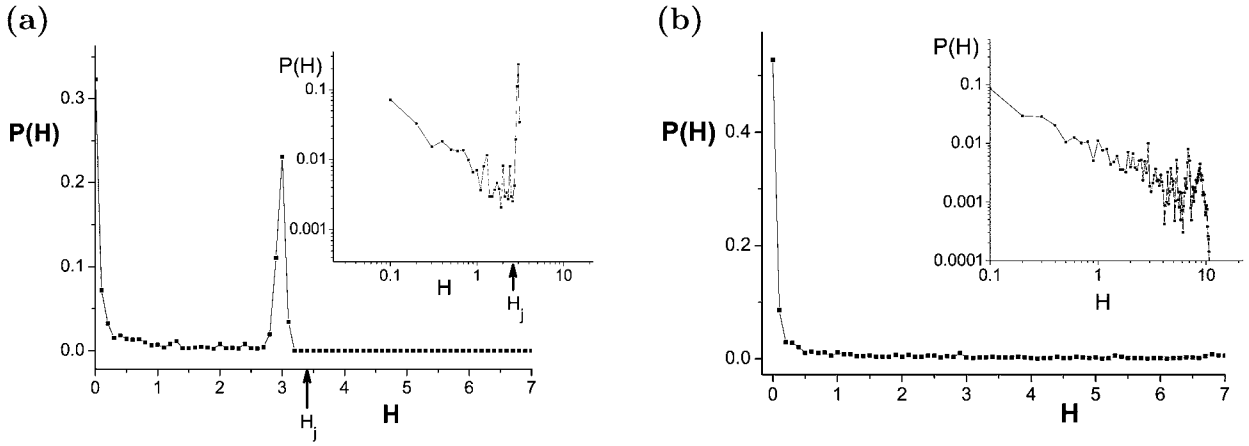

FIG. 10. Histograms of the probability density as a function of H, for a two-patch LV system with only prey diffusion ($D_b=1, D_a=0$) (b) and only predator diffusion ($D_a=1, D_b=0$) (a). Both systems were subject to demographic stochasticity, modeled by a multiplicative noise proportional to the square root of the population density. In both cases, the probability density is concentrated around $H=0$; however, Jansen's instability manifests itself in the peak at the instability radius at the left panel, caused by the "reflection" from the unstable manifold (note the arrow that indicates the first unstable orbit). The log-log plots of that histogram (insets) show that the tail of the distribution is continuous at the right panel, but the probability to find the system with H above the instability limit is practically zero. The LV parameters are $\mu=\sigma=1$ and $\lambda=10^{-5}$.

only for relatively large diffusivities, where the effect of amplitude-induced instability is suppressed by patches of synchronization.

Another factor which is important for the observation of the effects of phase instability is the noise amplitude. As Jansen's instability is linear, it must dominate the system if the noise level is very small. However, the level of noise in a real system is bounded from below by demographic stochasticity, the intrinsic noise that should appear in any system independent of environmental factors. The relative strength of this noise scales with $1/\sqrt{N}$, where N is the number of individuals. One thus expects that the effects associated with the linear instability will manifest themselves strongly if the size of the population is large. This effect is demonstrated in Fig. 9, where the probability distribution to find the system at H is plotted versus H for two-patch system with different population sizes and multiplicative noise. For small population size (relatively large noise) other mechanisms stabilize the system far from Jansen's limit, dense systems flow away and stabilize only due to the linear effect.

In the relevant multiplicative noise levels (dense limit) one may also compare the two opposite cases of no predator migration (where one should expect angular instability), and no prey diffusion, where no such instability is present. Figure 10 clearly shows the stabilizing effect of angular-induced desynchronization. The populations are stable in both regimes, but the instability cuts the tail of the distribution, leaving only a peak close to the "reflecting boundary."

To conclude, it has been shown that systems where only the predator admits the ability to migrate (canonical examples include herbivore—plant or parasite insect—plant systems, like the famous biological control of the Prickly Pear cactus by the moth *Cactoblastis cactorum* in eastern Australia [14]) may support sustained oscillations in noisy environments. This phenomenon has been explained here, and its cause was traced to the dependence of the angular velocity on the azimuthal angle along an orbit lying in the homogenous manifold. This insight allows us to incorporate that phenomenon into a generic framework of coupled nonlinear oscillators and to compare that mechanism with other stabilizing effects. In a separate publication [15], we intend to put forward a general classification scheme for stable population oscillations, a scheme that may be used to typify the observed desynchronization-induced stable manifold according to its underlying mechanism.

This work was supported by the CO3 STREP of the Complexity Pathfinder of NEST (EC FP6). We thank Arkady Pikovsky, Vincent Jansen, and A. M. de Roos for useful discussions and comments.

[1] A. J. Lotka, Proc. Natl. Acad. Sci. U.S.A. **6**, 410 (1920); V. Volterra, *Lecon sur la Theorie Mathematique de la Lutte pour le via, Gauthier-Villars*, Paris, 1931; J. D. Murray, *Mathematical Biology* (Springer, New-York, 1993).

[2] G. F. Gause, *The struggle for existance* (William and Wilkins, Baltimore, 1934); D. Pimentel, W. P. Nagel, and J. L. Madden, Am. Nat. **97**, 141 (1963); C. B. Huffaker, Hilgardia **27**, 343 (1958).

[3] A. J. Nicholson, J. Anim. Ecol. **2**, 132 (1933).

[4] L. S. Luckinbill, Ecology **55** 1142 (1974); B. Kerr *et al.*, Nature **442**, 75 (2006); M. Holyoak and S. P. Lawler, Ecology **77**, 1867 (2000).

[5] D. J. D. Earn, S. A. Levin, and P. Rohani, Science **290** 1360 (2000); B. Blasius, A. Huppert, and L. Stone, Nature **399** 354 (1999).

[6] See a recent review by C. J. Briggs and M. F. Hoopes, Theor Popul. Biol. **65**, 299 (2004).

[7] V. A. A. Jansen, Oikos **74**, 384 (1995).

[8] V. A. A. Jansen and A. M. de Roos, in *The Geometry of Ecological Interactions: Simplifying Spatial Complexity*, edited by U. Dieckmann, R. Law, and J. A. J. Metz (Cambridge University Press, Cambridge, 2000), p. 183.

[9] V. A. A. Jansen and K. Sigmund, Theor Popul. Biol. **54**, 195 (1998).

[10] D. T. Gillespie, J. Phys. Chem. **81**, 2340 (1977).

[11] For extention of that treatment to many coupled patches see Refs. [8,9].

[12] See, e. g., H. D. I. Abarbanel, *Analysis of observed chaotic data* (Springer, Berlin, 1995), p. 87.

[13] R. Abta, M. Schiffer, and N. M. Shnerb, Phys. Rev. Lett. **98**, 098104 (2007).

[14] D. B. Freeman, Geogr. Rev. **82**, 413 (1992).

[15] R. Abta, A. Ben-Ishay, M. Schiffer, and N. M. Shnerb, e-print arXiv:q-bio.PE/0701032.